

Electrically driven metal-insulator transition in layered transition-metal dichalcogenides

R. Könenkamp

Hahn-Meitner-Institut-Berlin, Bereich Strahlenchemie, Glienicker Strasse 100, 1000 Berlin 39, West Germany

(Received 13 January 1988; revised manuscript received 21 March 1988)

A metal-insulator transition is reported for $\text{Mo}_x\text{W}_{1-x}\text{Se}_2$ single crystals in the compositional range $0 \leq x \leq 1$. The transition can be driven by the application of an electric field and is accompanied by large changes in the optical properties. Bistability in dark and photoconduction as well as in the reflectivity is observed in a wide temperature range in the vicinity of the transition.

Transition-metal dichalcogenide (MX_2) materials have attracted wide research interest due to their unusual structural properties. Many of these compounds crystallize in sheets of hexagonally coordinated atoms stacked in the sequence $X\text{-M-X}$, $X\text{-M-X}$. Within each of the layers the atoms are bonded covalently while the interlayer forces are of the van der Waals type. The resulting strong anisotropy has made these materials an interesting model system for the study of electronic¹ and ionic transport, intercalation,² superconductivity,³ and many other physical properties.⁴ Detailed structural studies have revealed that a number of stacking polytypes are possible in this class of materials. For the particular case of MoSe_2 a structural phase transition has been reported to occur at a pressure of 40 kbar and a temperature of 1500 K.⁵ In this paper we present—for the first time—evidence for a metal-insulator transition in the system $\text{Mo}_x\text{W}_{1-x}\text{Se}_2$, which can be activated by application of an electric field over a wide range in temperature at normal pressure. It is shown that this transition involves the bulk volume of the crystal and is accompanied by several novel electrical and optical phenomena.

Undoped single crystals of the layer-type compound $\text{Mo}_x\text{W}_{1-x}\text{Se}_2$ with compositions $x = 0, 0.25, 0.5, 0.75$, and 1 were prepared from mixtures of MoSe_2 and WSe_2 powders in high-temperature solutions of Te and Se, or by chemical-vapor transport. The crystals obtained had the shape of thin plates with an area of $\sim 1 \text{ mm}^2$ and thickness $< 100 \mu\text{m}$. X-ray powder diffractograms indicated the hexagonal structure type $P6_3/mmc$. X-ray fluorescence measurements confirmed that the stoichiometry of the crystals corresponded to the mixing ratio of the powders. Thermoelectric power measurements showed that the crystals had n -type conductivity. Further details of the preparation and characterization have been given in previous publications.⁶ Electrical contacts were usually made using silver paste, but a variety of other materials including Pt and Al in pastes or as solids were found to yield similar results, demonstrating that intercalation had no bearing on the experiments. The samples were mounted in good thermal contact to a copper sample holder, serving as a heat sink, and cooled in a N_2 -exchange-gas cryostat.

Figure 1 shows an Arrhenius plot of the electric current in MoSe_2 for electric fields in the range 10^{-1} – 10^3

V/cm. For the lower electric field strengths the current behavior is Ohmic and the temperature dependence is exponential with an activation energy $E_A = 0.4 \text{ eV}$. The low-field curves can therefore be associated with the customarily investigated semiconducting phase of the material. In the higher electric field range, $\epsilon > 10 \text{ V/cm}$, the current is seen to rise superlinearly with field. This behavior has also been noted by other researchers and was attributed to carrier injection from the contacts.⁷ A comparison of the injected and thermal carrier concentrations supports this explanation for the temperature regime $T < 250 \text{ K}$, and a shift of the quasi-Fermi-level to 0.25 eV below the conduction-band edge can be estimated for the higher fields applied here.⁸ However, injection is insufficient to explain the observed metallic behavior for

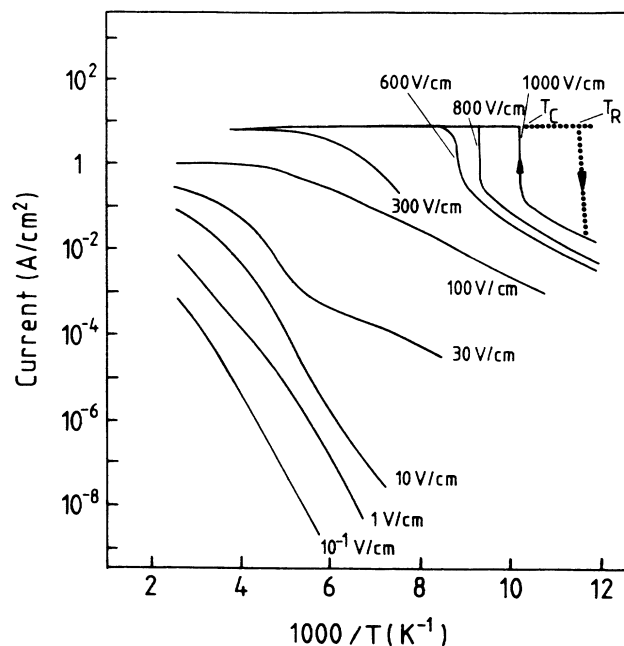


FIG. 1. Current density vs inverse temperature for various electric fields applied parallel to the crystal layers.

$T > 150$ K and $\epsilon > 600$ V/cm, which sets in at a critical set of conditions, T_c and ϵ_c , with an instantaneous rise in current. When T_c is passed by lowering the temperature, the current behavior remains metallic, establishing a new branch in the diagram (drawn as a dotted line) and the current eventually drops to the low-conductivity branch at a temperature T_R . The bistable regime between T_c and T_R can be observed over time periods $t > 1$ h. The most interesting feature of the described transition is the electric field dependence illustrated in Fig. 2, where the current-voltage dependence is plotted for various temperatures. At the passage of a critical electric field the current rises by more than an order of magnitude and remains at this level until the field is reduced to a value $\epsilon_R < \epsilon_c$, where it drops to the low-conductance branch. We find a well-defined bistable regime between ϵ_c and ϵ_R whose width increases for lower temperatures. The hysteresis can be multiply reproduced in a single sample and was observed in a similar fashion for all the $\text{Mo}_x\text{W}_{1-x}\text{Se}_2$ compositions mentioned above. The typical time scale for the transition is ~ 100 ms. The transition is observed with coplanar as well as with sandwich-type contact configuration, i.e., with the electric field parallel or perpendicular to the layers.

Figures 2(b) and 2(c) show the dependence of the photoconductivity and reflectivity on the applied electric field. The behavior of the photoconductivity is qualitatively similar to that of the dark current in Fig. 2(a), and shows a hysteresis over the same field interval. However, the metallic branch exhibits a region of negative differential photoresistance which can repeatedly be observed in both voltage-sweep directions. Bistability with relative differences of more than 20% in the two branches is also observed in the reflectivity. The optical changes can be observed over a wide wavelength interval, $800 < \lambda < 1100$ nm. In spectrally resolved measurements a shift in the interference pattern by a similar amount is observed, indicating that the dielectric constant changes in the transition.

Since the conductivity in the metallic regime is well below that of ordinary metals, principally two different

explanations for the metallic state must be considered. These involve either a low-mobility conduction mechanism⁹ in the metallic state or a small volume contribution of the metallic conductivity as in the electrical threshold switching of glassy and amorphous semiconductors.¹⁰ Clearly, if only a small line-shaped subvolume undergoes a transition to a highly conductive state, the changes in photoconductivity and reflectivity should be small, and they should be negative for the photoconductivity and positive for the reflectivity. Figures 2(b) and 2(c) demonstrate that this is not the case, and we are led to conclude that the transition involves the crystal bulk.

In Fig. 3 the spectral dependences of the photoconductivity for the low- and high-conductance states are shown. The two spectra were recorded at the same temperature and electric field, the only difference being that the state of the sample corresponded to the two different branches in the bistable regime. The solid line in Fig. 3, showing the spectrum for the semiconducting state at $T = 82$ K, agrees with published spectra for MoSe_2 obtained by similar methods. These also show an excitonic peak at $E = 1.55$ eV,^{11,12} corresponding to the peak at ~ 830 nm. The dotted line represents the metallic state after renormalization at wavelength $\lambda = 700$ nm. Over the whole wavelength interval the photoconductivity for the metallic state is larger by approximately a factor 20. This is linked to an increase of the photocarrier lifetime rather than the carrier mobility. This is demonstrated in the inset of the figure which shows the photoconductive decay after an 8-ns laser-pulse excitation. A more detailed analysis of the decay process reveals a change in the recombination kinetics from bimolecular behavior in the semiconducting state to monomolecular characteristics in the metallic state. The absorption tail in the high-conductance state is shifted to lower energies by ~ 0.1 eV and a corresponding shift of ~ 0.15 eV is observed for the exciton peak. The broadening of the shifted exciton peak can be attributed to Thomas-Fermi screening by free carriers.

These observations can be fitted in a consistent model, which we will outline in the following. The pronounced

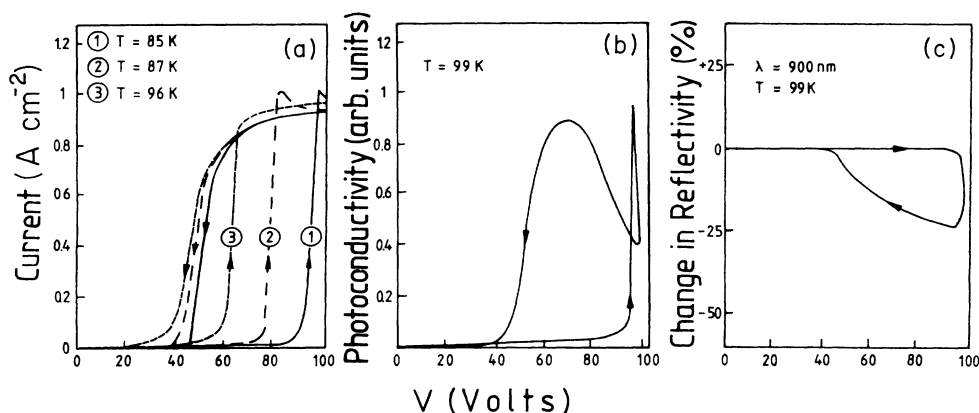


FIG. 2. (a) Current density vs voltage for MoSe_2 at various temperatures near the transition. (b) Photocurrent vs voltage for MoSe_2 . (c) Relative reflectivity change vs voltage for MoSe_2 .

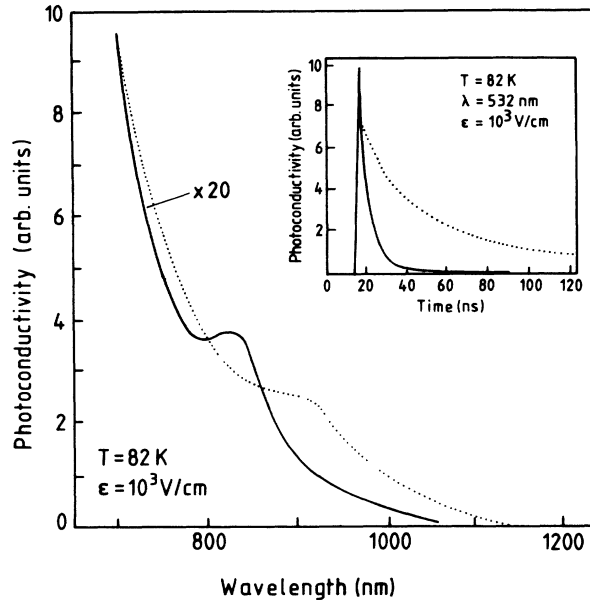


FIG. 3. Photocurrent spectra for MoSe₂ in the metallic state (dotted) and the semiconducting state (solid). Inset: photoconductive decay after an 8-ns laser pulse.

spectral changes in reflectivity and photoconductivity show that the band structure of the metallic and semiconducting states are different from each other. Since all of the bulk crystal is involved in the transition it is likely that structural rearrangements are the cause of the transition. This idea agrees with the observed slowness of the transition, and is supported by preliminary results from Laue-diffraction measurements, which will be reported in the near future.¹³ Further, it allows for a straightforward explanation of the bistable behavior, if one assumes that the metallic state is a metastable alteration of the known semiconducting state. The remaining strong photoconductivity in the metallic state is a clear indication for the survival of an energy gap, which is narrower by 0.1–0.15 eV as evidenced by the shifted absorption tail and exciton peak. It appears plausible that the narrowed band gap comprises new electronic states, such as band-tail-like and defect states as a consequence of the structural changes. The emergence of these states will shift the Fermi energy and this is evidently the reason for the observed changes in recombination. Moreover, if these states have a sufficiently high density they will allow for a sizable contribution to the electronic transport by a tunneling-like mechanism as typically observed in Anderson transitions. The characteristic of the transport is metallic since it occurs at the Fermi energy, but the carrier mobility is low due to the small transfer integral among the sites.⁹ This explains the comparably low dark conductivity, while at the same time, it allows for the occurrence of photoconduction due to the promotion of excess carriers above the band edge.

To elucidate the role of the electric field in the transition we have investigated the temperature dependence of the transition in more detail using the reflectivity as the measured parameter since it has the weakest temperature dependence. Figure 4 shows that the transition is abrupt

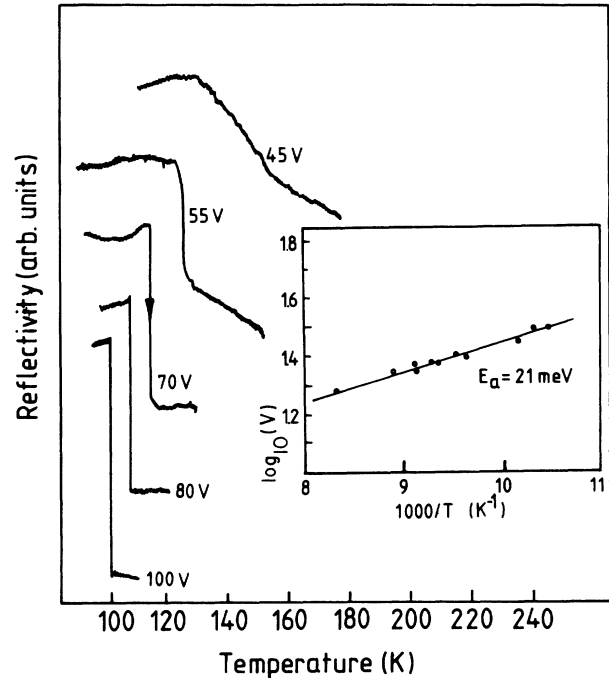


FIG. 4. Reflectivity vs temperature at various electric fields; contact separation is ~ 1 mm. Inset: Arrhenius plot of parameters ϵ_c and T_c .

only at higher fields while it becomes somewhat sluggish at fields of $\epsilon < 500$ V/cm. The relationship between the critical parameters ϵ_c and T_c plotted in the inset of the figure is temperature activated with $E_a = 0.021$ eV. This behavior is not compatible with concepts such as barrier lowering or an increased carrier energy.¹⁴ Instead, a possible explanation for this behavior can be based on the assumption that the transition between the two states involves an energy barrier and that the rate of the transition is proportional to a field-dependent factor and the Boltzmann term, i.e., $R \propto f(\epsilon) \exp(-E_a/kT)$, with f some algebraic function of the electric field. As seen from Fig. 1 the transition is only observed under high injection conditions and no indication for a transition was detected with blocking contacts. This suggests that the field dependence for the rate is linked to the charge carrier density in the crystal. In the case of one-carrier injection the electric charge is directly proportional to the applied field,⁸ $f(\epsilon)$ is linear in ϵ , and the activation energy of 21 meV corresponds to the barrier height for the transition. Qualitatively, such an interpretation is indeed borne out in Fig. 1, where a tendency toward metallic conduction is noted at $T > 250$ K, even at lower fields. Also, the broadening of the transition at higher T as noted in Fig. 4 is in agreement with thermal activation. Much of the structural work on transition-metal dichalcogenides had indicated a strong electron-phonon coupling in these materials. It is now well documented that in some systems charge transfer to the metal d band can lead to a metal-insulator and structural transition by a coupling of charge-density waves to the crystal lattice. The charge transfer can—in some cases—be mediated by intercalation of appropriate electron donors.

Intercalation-driven metal-insulator transitions have indeed been observed in group-VI transition-metal dichalcogenides using alkali-metal intercalates,¹⁵ but it is generally assumed that there is little or no structural distortion within the host crystal layers. This is possibly due to counteracting effects accompanying the intercalation process, such as a stiffening of the phonon spectrum and a narrowing of the conduction band in the host material.² Charge transfer without the introduction of foreign atoms, however, as achieved here by electron injection is not accompanied by such effects and may thus induce structural lattice distortions. These may then, in turn, explain the field-dependent effects as described above. More recently, studies of the dynamic properties of charge-density waves have shown that hysteretic and nonlinear conductivity can also result from a motion of the charge-density wave system itself. Clearly, more

research is needed to determine the microscopic mechanism involved in the transition.

To conclude we have presented evidence for an electrically driven metal-insulator transition in layered transition-metal dichalcogenide single crystals. The transition involves a change in the band structure and a low-mobility transport process for the metallic state. The transition is accompanied by large changes in the photoconductivity and reflectivity and it gives rise to a well-defined regime of electrical and electrooptical bistability. A tentative model was presented which accounts for the qualitative features of the observed effects.

It is a pleasure to acknowledge the provision of the samples by Dr. W. K. Hofmann, the technical assistance of Ms. Sophie Krebs, and helpful discussions with Professor H. Tributsch.

¹R. Fivaz and E. Moser, *Phys. Rev.* **163**, 743 (1967).

²R. H. Friend and A. D. Yoffe, *Adv. Phys.* **36**, 1 (1987).

³R. B. Somoano and A. Rembaum, *Phys. Rev. Lett.* **27**, 402 (1971).

⁴J. A. Wilson and A. D. Yoffe, *Adv. Phys.* **18**, 193 (1969).

⁵L. C. Towle, V. Oberbeck, B. E. Brown, and R. E. Stajdohar, *Science* **15**, 895 (1966).

⁶W. K. Hofmann, R. Könenkamp, Th. Schwarzlose, M. Kunst, H. Tributsch, and H. J. Lewerenz, *Ber. Bunsenges. Phys. Chem.* **90**, 824 (1986).

⁷T. J. Wieting and A. D. Yoffe, *Phys. Status Solidi* **37**, 353 (1970).

⁸M. A. Lampert and P. Mark, *Current Injection in Solids* (Academic, New York, 1970).

⁹N. F. Mott and E. Davis, *Electronic Processes in Non-Crystalline Materials* (Clarendon, Oxford, 1979).

¹⁰D. Adler, H. K. Henisch, and N. F. Mott, *Rev. Mod. Phys.* **50**, 209 (1978).

¹¹K. K. Kam and B. A. Parkinson, *J. Phys. Chem.* **86**, 463 (1982).

¹²P. M. Amirtharaj, F. H. Pollak, and A. Wold, *Solid State Commun.* **41**, 581 (1982).

¹³S. Fiechter and R. Könenkamp (unpublished).

¹⁴See, for example, K. Seeger, *Semiconductor Physics* (Springer-Verlag, Berlin, 1973).

¹⁵J. V. Acrivos, W. Y. Liang, J. A. Wilson, and A. D. Yoffe, *J. Phys. C* **4**, L18 (1971).